Seasonal climate summary for the southern hemisphere (winter 2016): a strong negative Indian Ocean Dipole brings wet conditions to Australia

Blair Trewin

Bureau of Meteorology, Australia

(Manuscript received June 2018; accepted June 2018)

This is a summary of the southern hemisphere atmospheric circulation patterns and meteorological indices for winter 2016; an account of seasonal rainfall and temperature for the Australian region and the broader southern hemisphere is also provided. One of the strongest negative phases on record of the Indian Ocean Dipole (IOD) developed during the season, contributing to Australia's second-wettest winter on record, with rainfall above average over the vast majority of the continent. Neutral conditions prevailed in the tropical Pacific following the end of a strong El Niño event in autumn 2016, but the continuing effect of the 2015-16 El Niño was still evident in southern hemisphere temperatures, which were at or near record high levels.

1 Introduction

This summary reviews the southern hemisphere and equatorial climate patterns for winter 2016, with particular attention given to the Australasian and equatorial regions of the Pacific and Indian ocean basins. The main sources of information for this report are analyses prepared by the Australian Bureau of Meteorology, the United States National Oceanic and Atmospheric Administration (NOAA) and the Global Precipitation Climatology Center (GPCC).

Unless otherwise stated, anomalies are calculated with respect to the period from 1961 to 1990, and percentile-based analyses for the period from the start of the relevant date set to 2017.

2 Pacific and Indian ocean basin climate indices

2.1 Southern Oscillation Index

The Troup Southern Oscillation Index[1] (SOI) for the period from January 2012 to August 2016 is shown in Figure 1, also shown is a five-month weighted, moving average of the monthly SOI.

[1] The Troup Southern Oscillation Index (Troup, 1965) used in this article is ten times the standardised monthly anomaly of the difference in mean sea level pressure (MSLP) between Tahiti and Darwin. The calculation is based on a sixty-year climatology (1933–1992), with records commencing in 1876. The Darwin MSLP is provided by the Bureau of Meteorology, and the Tahiti MSLP is provided by Météo France inter-regional direction for French Polynesia.

Corresponding author: Blair Trewin – Bureau of Meteorology, GPO Box 1289, Melbourne, Vic.,3001
Email: blair.trewin@bom.gov.au

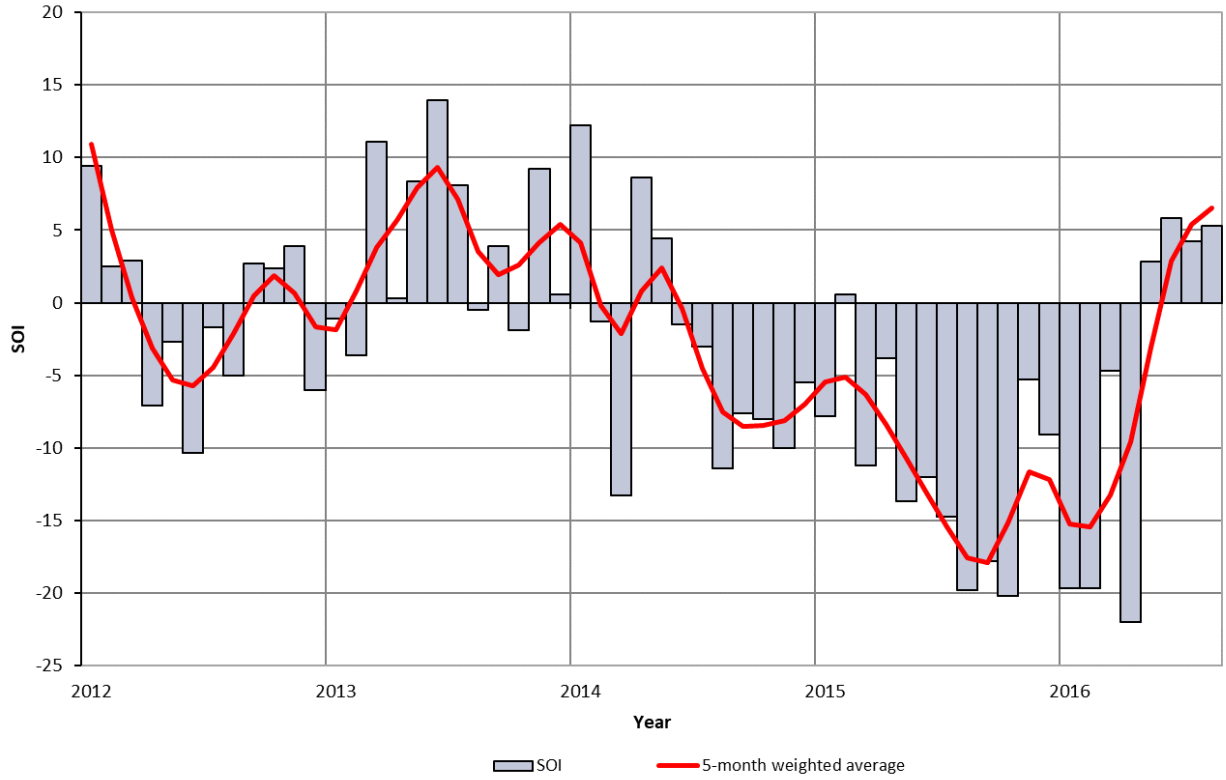

Figure 1 Troup Southern Oscillation Index (SOI) values from January 2012 to August 2016, with a five-month binomial weighted moving average.

Sustained negative values of SOI below −7 are often indicative of El Niño episodes while sustained positive values of SOI above +7 are typical of La Niña. Following a sustained period of strongly negative values during the 2015-16 El Niño event (Rosemond and Tobin, 2018), with the five-month average value of the SOI remaining below −10 from May 2015 to April 2016, the SOI rose to weakly positive values in May 2016 and remained weakly positive throughout winter 2016, consistent with neutral El Niño-Southern Oscillation (ENSO) conditions. The winter 2016 mean value of the SOI was +5.1, with the monthly values for June, July and August being +5.8, +4.2 and +5.3 respectively.

2.2 Composite monthly ENSO index (5VAR)

The El Niño–Southern Oscillation (ENSO) 5VAR Index[2] is a composite monthly ENSO index, calculated as the standardised amplitude of the first principal component of the monthly Darwin and Tahiti mean sea-level pressure (MSLP) and monthly indices NINO3, NINO3.4 and NINO4 sea-surface temperatures[3] (SSTs). Positive values of 5VAR that are in excess of one standard deviation are typically associated with El Niño, while negative 5VAR values below one standard deviation are indicative of La Niña.

The 5VAR index fell below +1 in May 2016 (Figure 2), consistent with the decline of El Niño and the onset of neutral ENSO conditions, and was near zero throughout winter 2016. Monthly values were +0.2 for June, −0.1 for July and −0.3 for August.

The NINO3.4 index, which measures SSTs in the central Pacific Ocean in a box covering 5 °N–5 °S and 120–170 °W, is used by the Australian Bureau of Meteorology to monitor ENSO. NINO3.4 is closely related to the Australian climate (Wang and Hendon, 2007). NINO3.4 values fell below zero early in winter 2016, having been positive since April 2014, and weekly

[2] ENSO 5VAR was developed by the Bureau of Meteorology and is described in Kuleshov et al. (2009). The principal component analysis and standardisation of this ENSO index is performed over the period 1950–1999.
[3] SST indices obtained from ftp://ftp.cpc.ncep.noaa.gov/wd52dg/data/indices/sstoi.indices.

values remained negative for most of the winter, with monthly mean values of −0.1 °C in June, −0.4 °C in July and −0.5 °C in August. However, the negative values during winter fell short of La Niña thresholds.

2.3 Indian Ocean Dipole (IOD)

The Indian Ocean Dipole (IOD)[4] (Saji et al., 1999) is the difference in sea surface temperature anomalies between the western node of the tropical Indian Ocean (centred on the equator) off the coast of Somalia and the eastern node off the coast of Sumatra. The Indian Ocean Dipole is said to be in a positive phase when values of the Dipole Mode Index (DMI) are persistently greater than +0.4 °C, neutral when the DMI is persistently between –0.4 °C and +0.4 °C and negative when DMI values are less than –0.4 °C.

When Australia is under the influence of a negative IOD phase, warm maritime air is driven eastwards across the continent, leading to negative IOD being associated with an increased chance of a wetter than average winter-spring for much of the continent.

The IOD entered a strong negative phase in late May 2016 and remained strongly negative thoughout winter 2016, driven largely by exceptionally warm conditions in the eastern node off Sumatra (Figure 7). Sea-surface temperatures in this region were at record or near-record high levels (Figure 8), whilst in the western node, off Somalia, sea-surface temperatures were close to average. Weekly DMI values (Figure 3) were below −0.5 °C throughout winter 2016, and fell below −1 °C in late June and most of July, reaching −1.37 °C in early July, making it one of the strongest negative IOD episodes on record (exact rankings of historical IOD events vary considerably between different data sets). This strong negative IOD phase is likely to have contributed substantially to the very wet winter in most of Australia (Section 9).

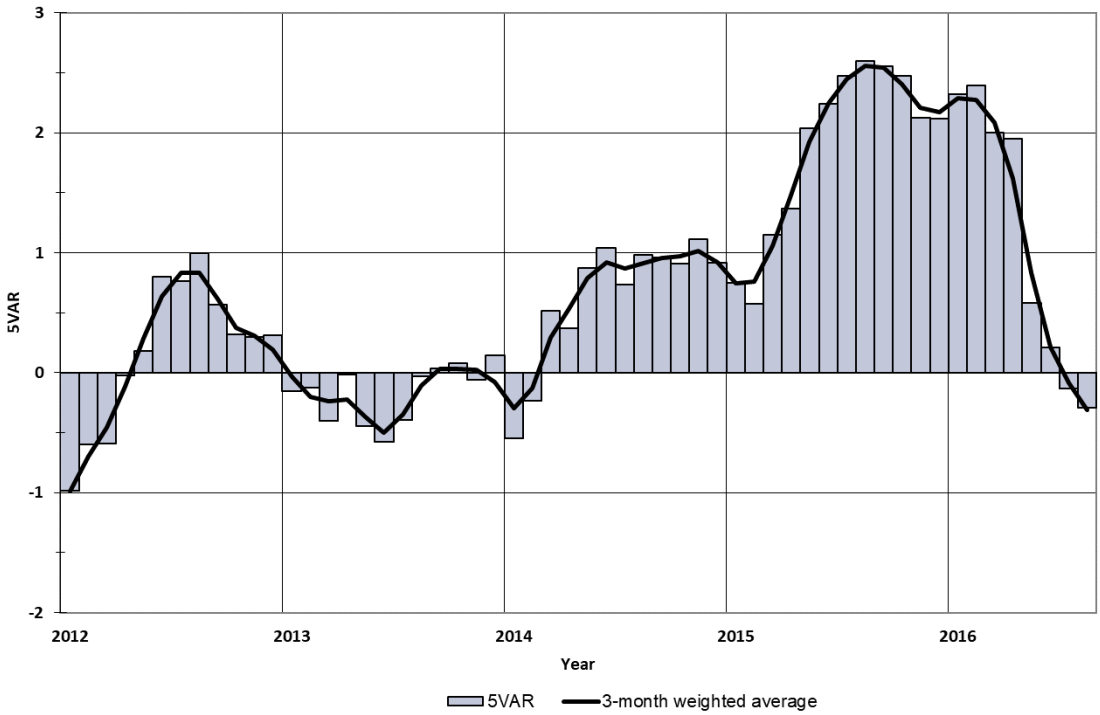

Figure 2 Values of the composite 5VAR ENSO index for the period January 2012 to August 2016 with the three-month binomially weighted moving average.

[4] http://www.bom.gov.au/climate/iod/. The western node is a box covering 10 °S to 10 °N, 50 °E to 70 °E, whilst the eastern node is a box covering 0° to 10 °S, 90 °E to 110 °E.

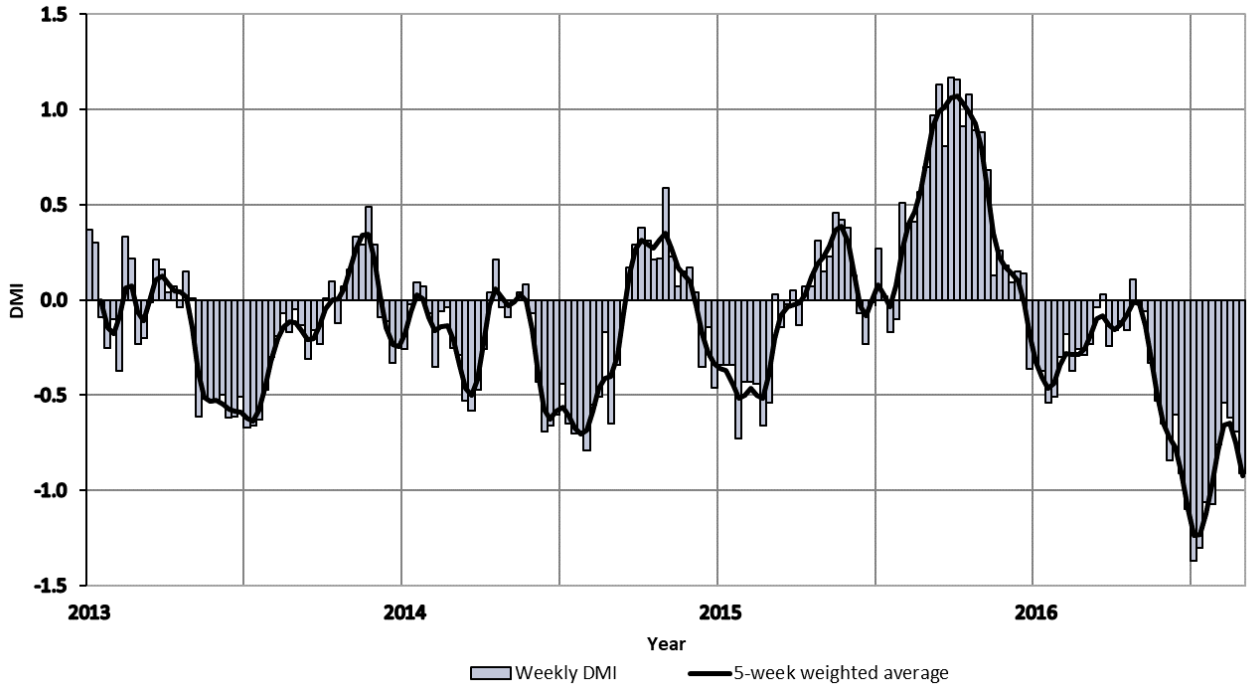

Figure 3 Weekly Dipole Mode Index (DMI) and five-week running mean from January 2013 to August 2016.

3 Outgoing longwave radiation (OLR)

Outgoing longwave radiation (OLR) in the equatorial Pacific Ocean can be used as an indicator of enhanced or suppressed tropical convection. Increased positive OLR anomalies typify a regime of reduced convective activity, a reduction in cloudiness and, usually, rainfall. Conversely, negative OLR anomalies indicate enhanced convection, increased cloudiness and usually increased rainfall. During La Niña, decreased convection (increased OLR) can be seen near the Date Line, while increased cloudiness (decreased OLR) near the Date Line usually occurs during El Niño. Similarly, when a negative IOD event is in place, OLR anomalies are negative over the eastern Indian Ocean where increased convection occurs.

The Hovmöller diagram of OLR anomalies along the equator from February to August 2016 (Figure 4) shows generally weak OLR anomalies near the dateline during the southern hemisphere winter 2016. These weak OLR anomalies follow the negative values which had prevailed in late summer and autumn during the latter phases of the 2015-16 El Niño event.

Averaged over an area at the International Date Line (7.5 °S–7.5 °N and 160 °E–160 °W), the standardised monthly OLR anomaly for June was +0.1, for July +0.5 and August +0.8.

Seasonal spatial patterns of OLR anomalies across the Asia-Pacific region between 40 °S and 40 °N for the southern hemisphere winter 2016 are shown in Figure 5. Negative OLR anomalies are evident over almost the entire Australian continent, with the strongest anomalies in a band extending from the central Northern Territory to southern inland Queensland, consistent with the near continent-wide wet conditions during the season. (It should, however, be noted that OLR values currently appear to have a negative bias over subtropical land areas, most likely associated with orbital decay of the GOES-18 satellite (Matthew Wheeler, pers. comm.)). An area of strongly negative OLR anomalies is also evident over the eastern IOD node off Java and Sumatra, extending over most of Java, consistent with a negative IOD.

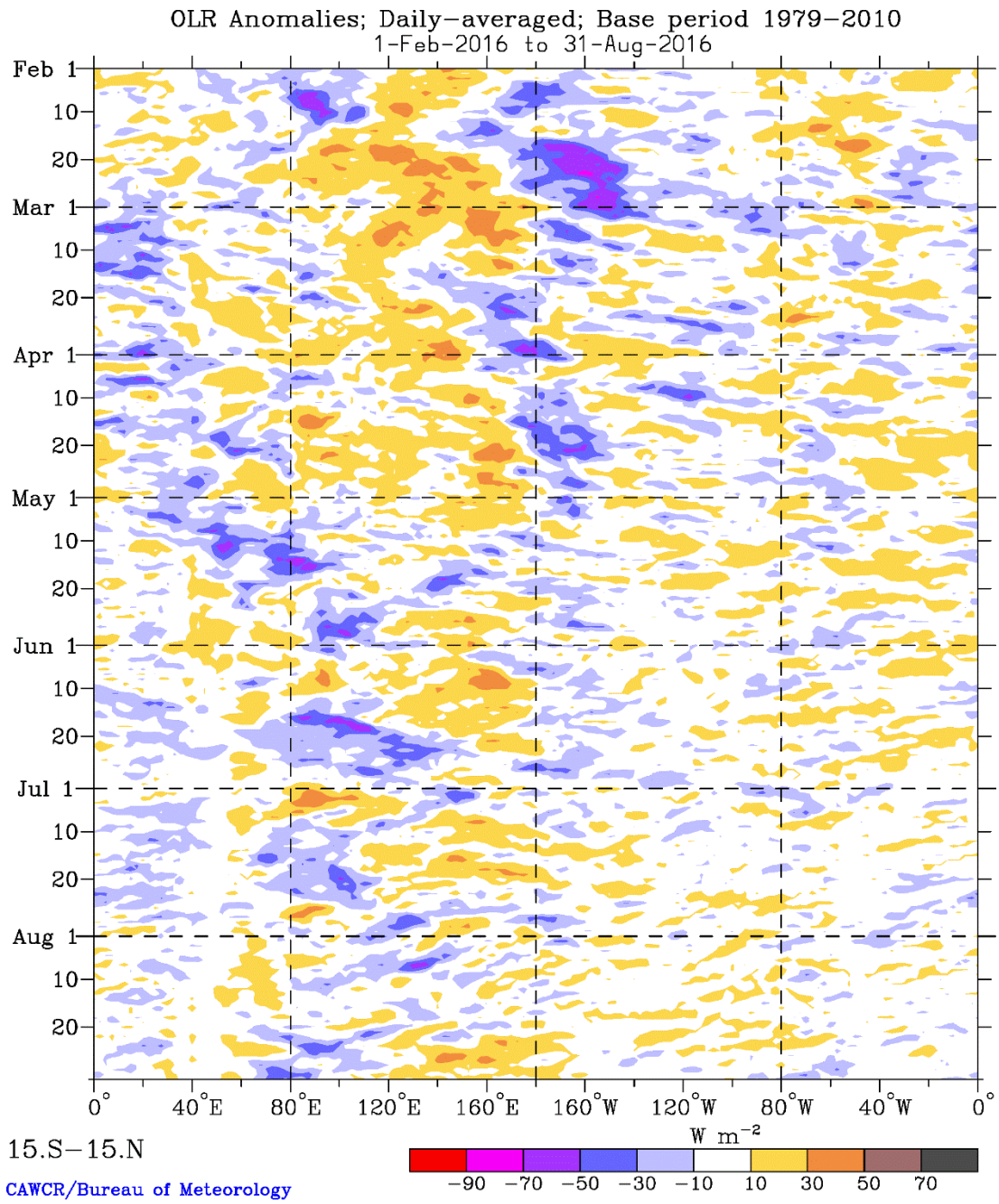

Figure 4 Time-longitude plot of outgoing daily-averaged long-wave radiation (OLR) anomalies, averaged over 15 °S-15 °N, for the period March to August 2016. OLR anomaly is from daily data with respect to a base period of 1979–2010, using interpolated OLR data provided by the NOAA/OAR/ESRL PSD, Boulder, Colorado, USA.

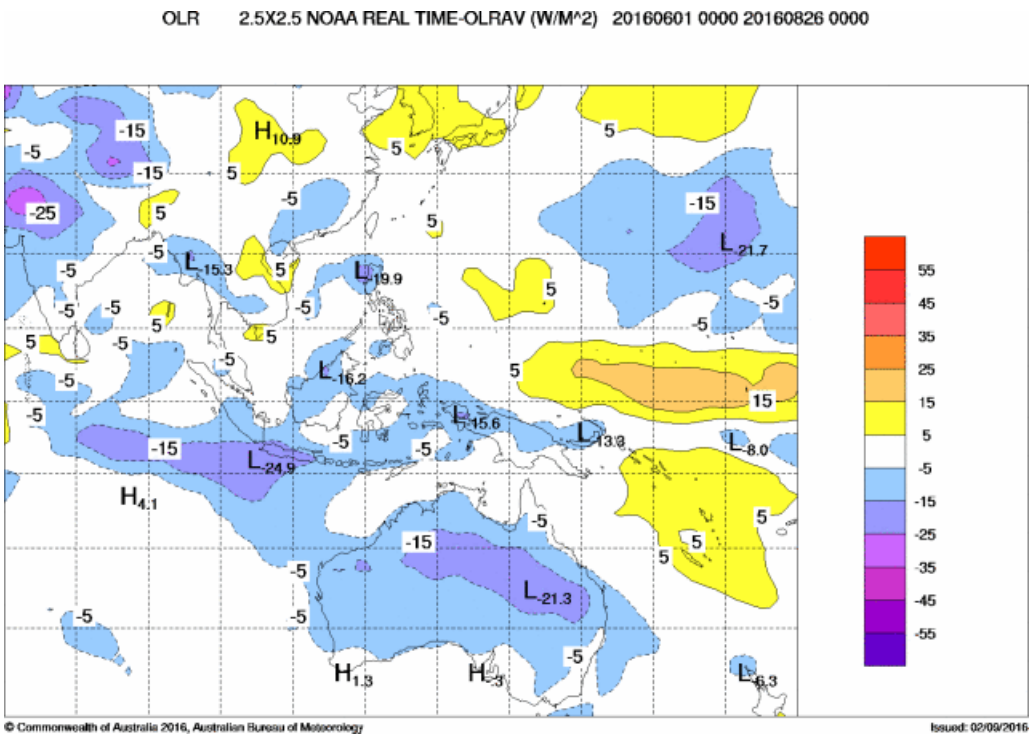

Figure 5 The OLR anomalies for the period from 1 June to 26 August 2016 (W m−2). Anomalies calculated with respect to base period 1979-2000.

4 Madden-Julian Oscillation (MJO)

The Madden-Julian Oscillation (MJO) is a tropical convective wave anomaly which develops in the Indian Ocean and propagates eastwards into the Pacific Ocean (Madden and Julian, 1971, 1972, 1994).The MJO takes approximately 30 to 60 days to reach the western Pacific, with a frequency of six to twelve events per year (Donald et al., 2004). When the MJO is in an active phase, it is associated with areas of increased and decreased tropical convection, with effects on the southern hemisphere often weakening during early autumn, before transitioning to the northern hemisphere. A description of the Real-time Multivariate MJO (RMM) index and the associated phases can be found in Wheeler and Hendon (2004).

The phase-space diagram of the RMM for winter 2016 is shown in Figure 6. A moderately active MJO phase prevailed for most of June. This moved into the Indian Ocean region in mid-June, coinciding with the onset of the southwest monsoon over the Indian subcontinent. MJO activity was then relatively weak for most of the remainder of the winter. MJO influences on Australian rainfall at multi-week timescales are generally modest at this time of year.

5 Oceanic patterns

5.1 Sea surface temperatures (SSTs)

The area-averaged sea-surface temperature for the southern hemisphere for winter 2016 was 0.66 °C [5] above the 20th century average. This was the warmest value on record in the NOAA dataset, surpassing the previous record set in 2015 by 0.03 °C.

Figure 7 shows sea surface temperature (SST) anomalies globally for winter 2016, relative to 1961-1990, whilst Figure 8 shows sea surface temperatures in the Australian region relative to the historical distribution. Sea surface temperatures were at least 1 °C above the 1961-1990 average over most of the Tasman and western Coral Seas, around Indonesia and in waters

[5] NOAA National Centers for Environmental Information, Climate at a Glance: Global Time Series, published May 2017, retrieved on May 13 2017 from http://www.ncdc.noaa.gov/cag/ (base period 1901-2000).

between Indonesia and Australia, locally reaching 2 °C above average near the coast of northwest Western Australia. Record high SSTs for the season occurred widely in Indonesian waters and off northwest Australia, as well as over much of the Tasman Sea and around the North Island of New Zealand.

SSTs were close to average in the equatorial Pacific east of the dateline, off the southwest of Western Australia, near the east coast of South America south of 20°S, and in the western Indian Ocean off the African coast, but elsewhere were at least 0.5 °C above average over most southern hemisphere waters north of 40 °S. Southern Ocean temperatures south of 40 °S were mostly close to average, although there was an area more than 0.5 °C below average around, and east of, the Drake Passage between South America and Antarctica.

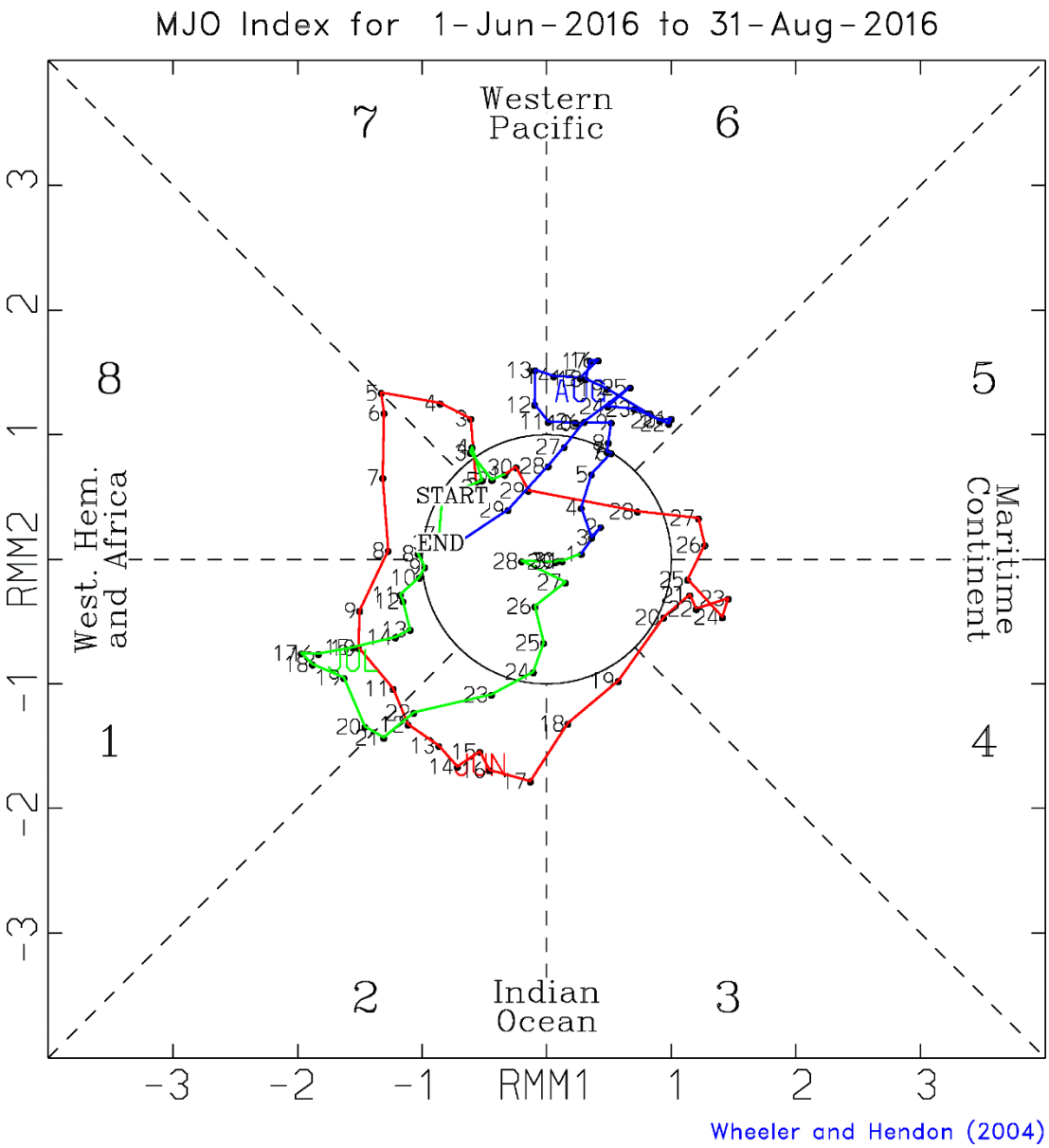

Figure 6 Real-time Multivariate MJO (RMM) phase-space diagram for winter 2016. Daily values are shown with June in red, July in green, and August in blue. The eight phases of the MJO and the corresponding (approximate) locations of the near-equatorial enhanced convective signal are labelled.

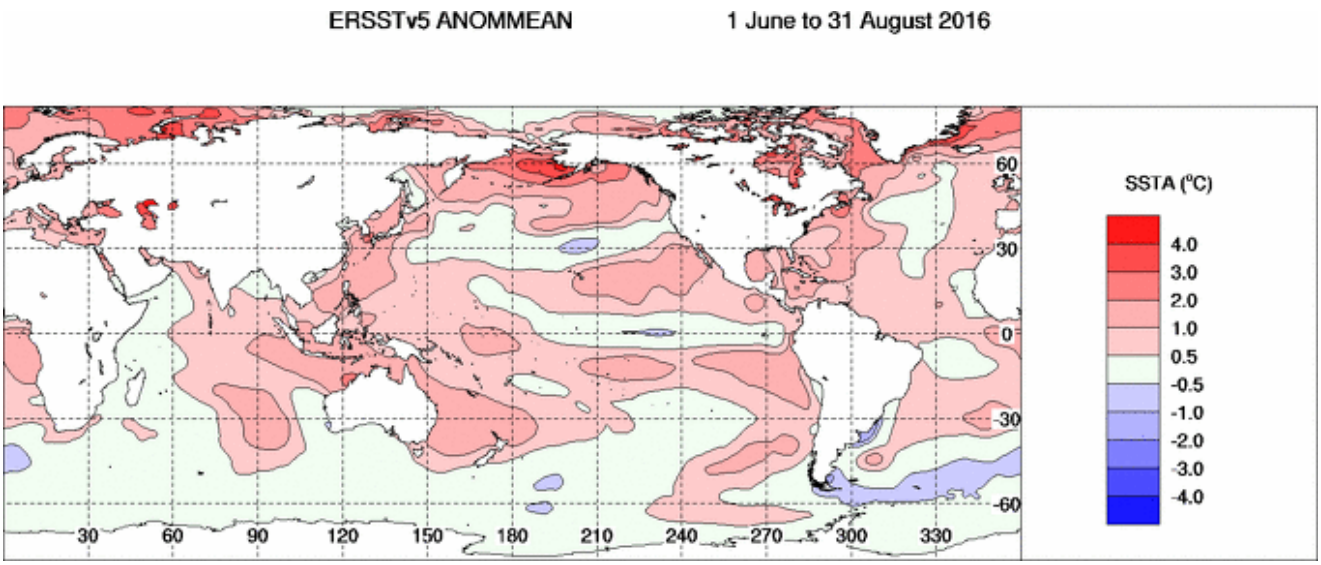

Figure 7 Global sea-surface temperature anomaly (°C) from 1961-1990 averages for austral winter 2016 (Extended Reconstructed Sea Surface Temperature Version 5 (ERSSTv5; Huang et al., 2017).

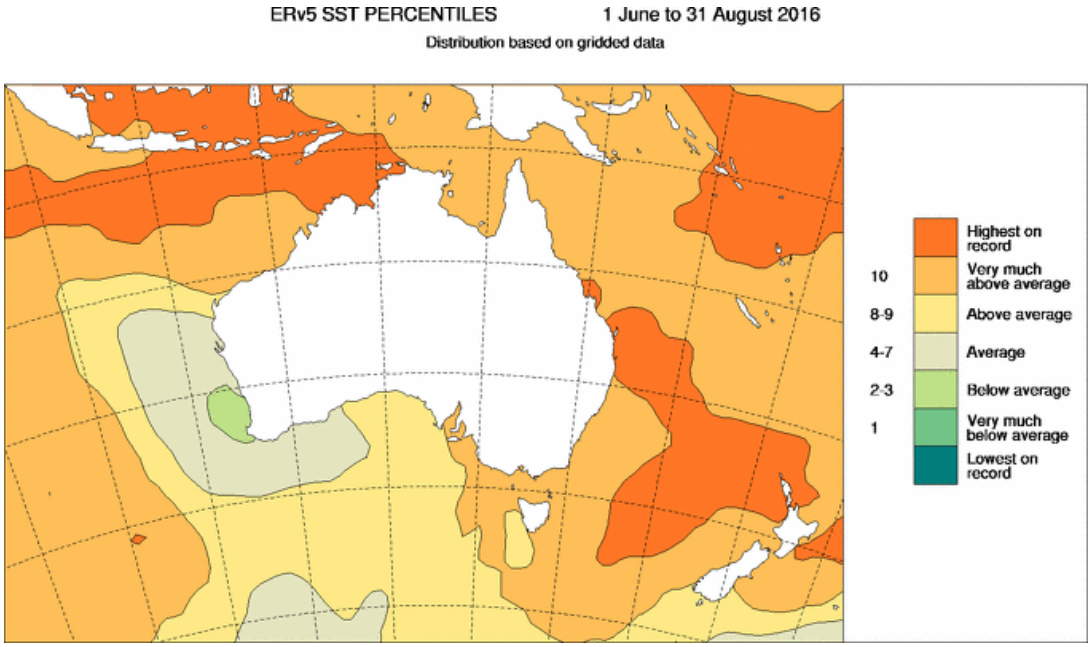

Figure 8 Sea-surface temperature (ERSSTv5) decile map of the Australian region for winter 2016.

5.2 Equatorial Sub-surface patterns

The 20 °C isotherm depth is generally located close to the equatorial thermocline, which is the region of greatest temperature gradient with depth and is the boundary between the warm near-surface and cold deep-ocean waters. Therefore, measurements of the 20 °C isotherm depth make a good proxy for the thermocline depth. Negative anomalies correspond to the 20 °C isotherm being shallower than average and is indicative of a cooling of sub-surface temperatures. If the thermocline anomaly is positive the depth of the thermocline is deeper. A deeper thermocline results in less cold water available for upwelling, and therefore a warming of sub-surface temperatures.

Sub-surface waters were generally cooler than average in the equatorial Pacific during the southern hemisphere winter 2016 (Figure 10). Accordingly, the thermocline was generally shallower than usual (Figure 9), except in the far east, where it was near average. The strongest sub-surface temperature anomalies were around −3 °C in August near 150 °W, modest compared with the anomalies seen in the early stages of some strong La Niña events. By August, weak warm anomalies were beginning to appear in the uppermost 50 metres in the western Pacific west of 160 °E.

6 Sea ice

Antarctic sea ice extent[6] during winter 2016 was very close to the 1981-2010 median throughout the season. The seasonal maximum of 18.44 million km^2 was reached on 31 August; the earliest seasonal maximum in the satellite record (which begins in 1979). The mean June, July and August extents (13.21, 15.97 and 17.81 million km^2 respectively) were all within 0.2 million km^2 of the respective medians. This follows a period of record or near-record high seasonal extents which ended during 2015. The northern edge of the sea ice during August was north of its mean climatological position between longitudes 45 °W and 10 °E (i.e., more ice than average), but was south of average between 70 and 140 °E, and between 80 and 140 °W (less ice than average).

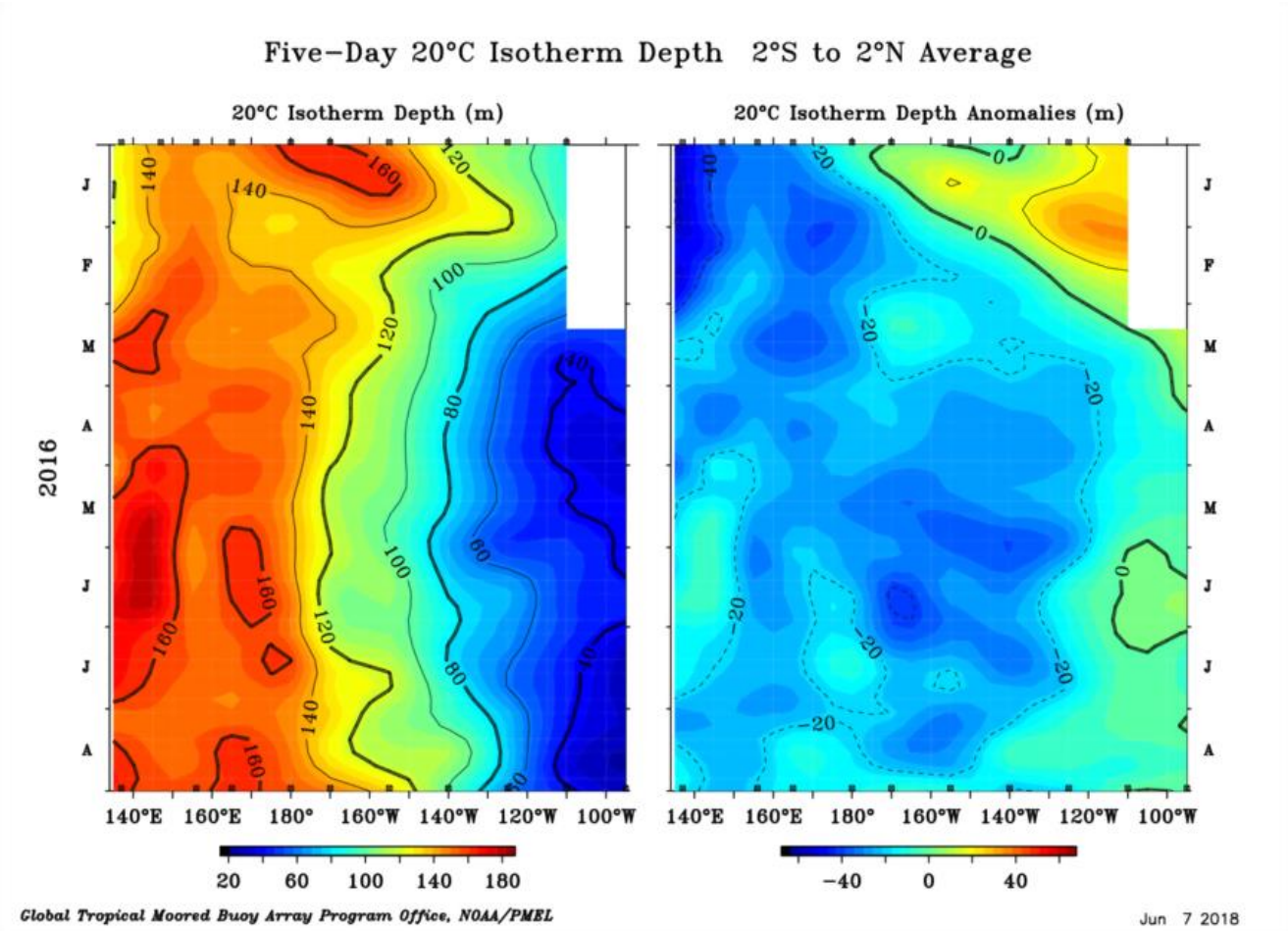

Figure 9 Hovmöller diagram of the 20 °C isotherm depth and anomaly along the equator from January 2016 to August 2016, obtained from NOAA's TAO/TRITON data[7].

[6] Sea ice information is sourced from the National Snow and Ice Data Center (http://www.nsidc.org).
[7] Hovmöller plot obtained from http://www.pmel.noaa.gov/tao/jsdisplay/

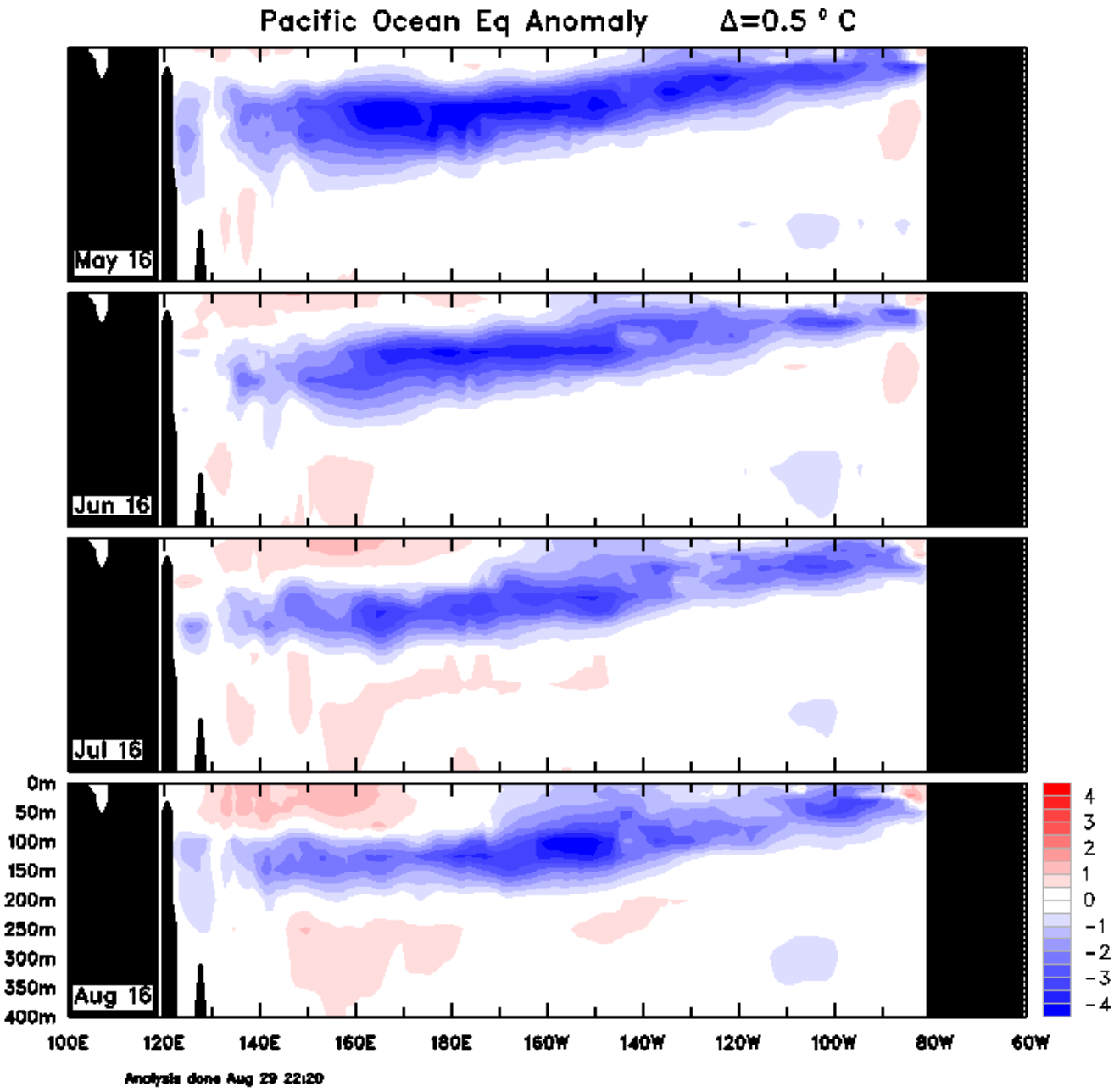

Figure 10 The cross-section of monthly equatorial sub-surface temperature anomalies from May 2016 to August 2016. Red shading indicates positive (warm) anomalies, and blue shading indicates negative (cool) anomalies.

7 Atmospheric circulation

7.1 Southern Annular Mode (SAM)

The Southern Annular Mode (SAM) was in a strongly positive phase during the early part of winter 2016, with index values above +1 from the start of June until 9 July. There was then a transition to a negative phase which persisted from about 28

July to 21 August, before a return to positive values to finish the season. Monthly mean values of the CPC SAM index were +2.57 for June (the highest June value in the post-1979 period), +0.41 for July and −0.74 for August.

Positive values of the SAM index in winter are associated with low rainfall in the southwest of Western Australia, southern Victoria and Tasmania, with only limited effects on winter rainfall in other parts of Australia (Hendon et al., 2007). South-west Western Australia and southern Victoria were amongst the less wet (relative to climatology) areas of Australia in June, although rainfall in these areas was still close to average.

For more information on the SAM index from the NOAA Climate Prediction Center (CPC), see http://www.cpc.ncep.noaa.gov/products/precip/CWlink/daily_ao_index/aao/aao.shtml.

7.2 Surface analyses

The mean sea level pressure (MSLP) pattern for winter 2016 is shown in Figure 11, computed using data from the 0000 UTC daily analyses of the Bureau of Meteorology's Australian Community Climate and Earth System Simulator (ACCESS) model[8]. MSLP anomalies are shown in Figure 12, relative to the 1979–2000 climatology obtained from the National Center for Environmental Prediction (NCEP) II Reanalysis data (Kanamitsu, 2002). The MSLP anomaly field is not shown over areas of elevated topography (grey shading).

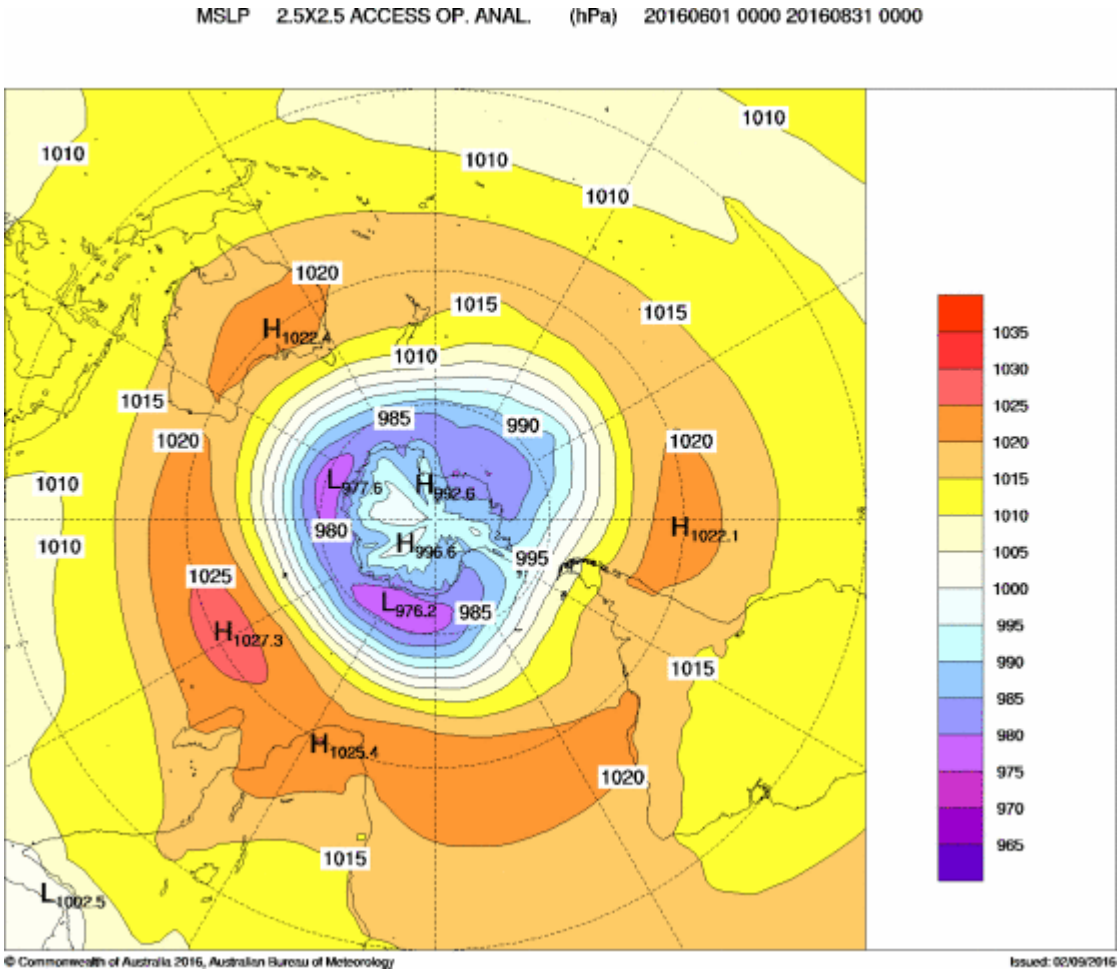

Figure 11 Southern hemisphere mean sea level pressure (MSLP) pattern for winter 2016.

[8] For more information on the Bureau of Meteorology's ACCESS model, see http://www.bom.gov.au/nwp/doc/access/NWPData.shtml

The seasonal mean sea level pressure anomaly analysis chart for winter 2016 (Figure 12) shows relatively weak MSLP anomalies over most of the southern hemisphere, with some evidence of the subtropical ridge extending further south than usual over the Indian Ocean, most prominent at around 75 °E. There is also a slight anomalous ridge near the southern tip of South America. MSLP anomalies were generally negative in the Antarctic sector with a prominent anomalous trough (with MSLP anomalies below −10 hPa) in the southeast Pacific near 50 °S 120 °W. MSLP was close to or slightly above average over most of Africa, South America, mainland Australia and New Zealand, although it was below average over Tasmania.

7.3 Mid-trophospheric analyses

The 500 hPa geopotential height, an indicator of the steering of surface synoptic systems across the southern hemisphere, is shown for winter 2016 in Figure 13. The associated anomalies are shown in Figure 14.

Geopotential height is valuable for identifying and locating features such as troughs and ridges which are the upper level equivalents of surface low and high pressure systems, respectively. Coinciding with the surface features discussed in Section 7.2, an anomalous trough is evident in the southeast Pacific near 120 °W, and anomalous ridging over southern South America and the Antarctic Peninsula. Positive 500 hPa geopotential height anomalies are evident over most subtropical regions, particularly over the oceans.

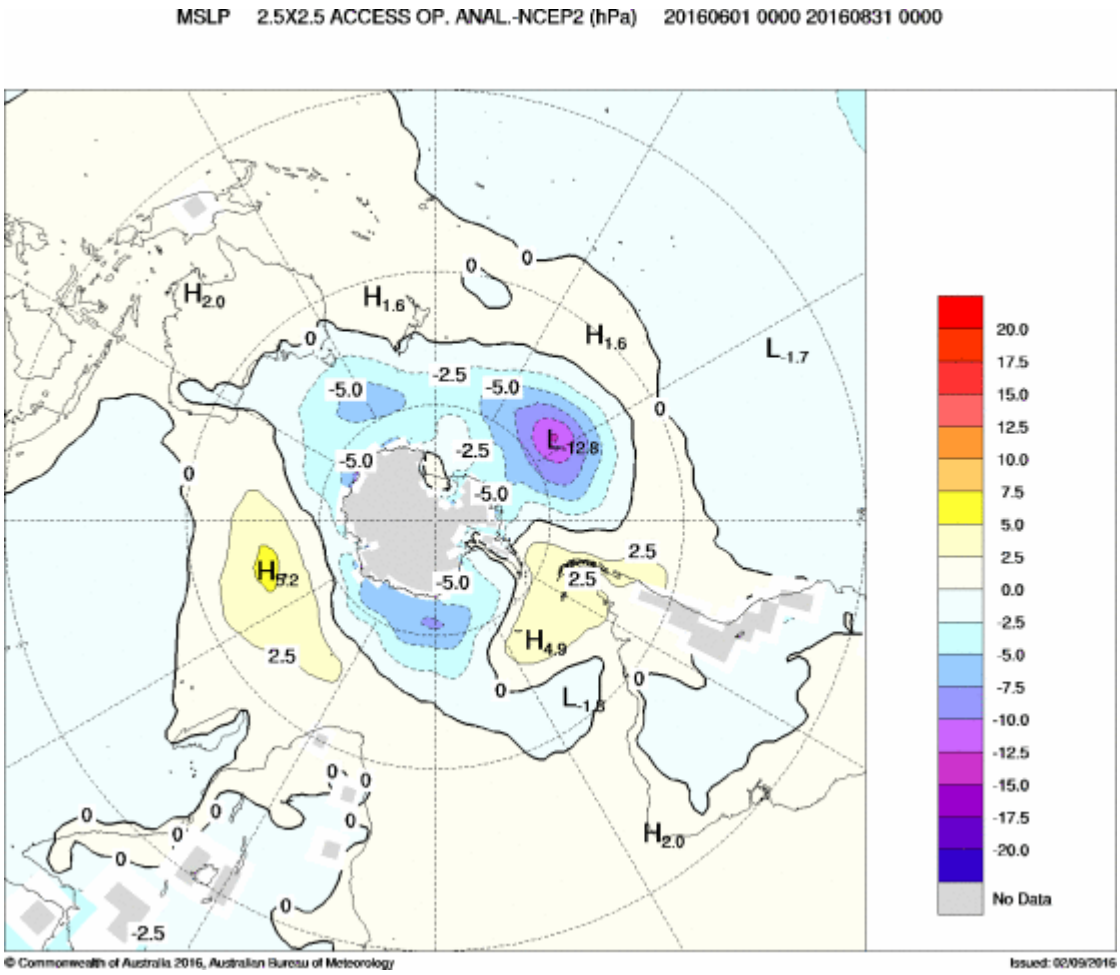

Figure 12 Southern hemisphere mean sea level pressure (MSLP) anomalies (hPa) for winter 2016. Anomalies calculated with respect to base period of 1979–2000.

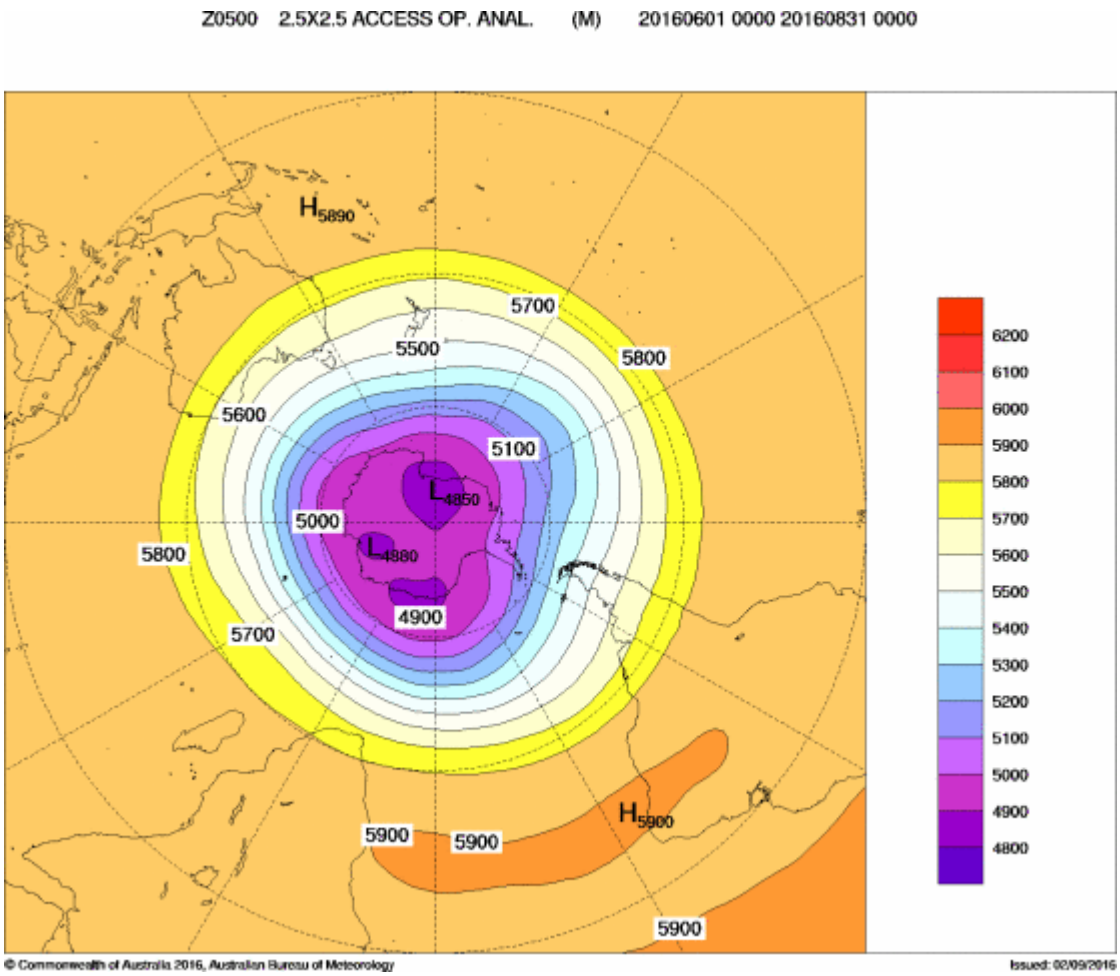

Figure 13 Winter 2016 500 hPa mean geopotential height (gpm).

8 Winds

Figures 15 and 16 show winter 2016 low-level (850 hPa) and upper-level (200 hPa) wind anomalies respectively. Winds are computed from ACCESS and anomalies with respect to the 22-year 1979–2000 NCEP climatology. Isotach contours are at an interval of 5 ms^{-1}.

Generally weak 850 hPa wind anomalies are evident in the Australian region, with the most substantial anomalies being northerly anomalies near the east coast, and westerly anomalies in the vicinity of Tasmania. Anomalies are also mostly relatively weak over the broader southern hemisphere. The strongest 850 hPa wind anomaly signal is an area of westerly anomalies near 40 °S 120 °W, on the northern side of the anomalous surface trough noted in Section 7. Westerly anomalies were present through much of the equatorial Indian Ocean, with weak anomalies in the equatorial Pacific; these anomalies are consistent with the climate states in the respective ocean basins (i.e., negative IOD and neutral ENSO). At the 200 hPa level, westerly anomalies were present through much of the southern hemisphere in the latitude band 30 to 40 °S, consistent with a stronger subtropical jet stream than average, with the largest anomalies found to the west of Western Australia. An area of positive anomalies near 40 °S 150 °W is consistent with a slight southward displacement of the subtropical jet stream.

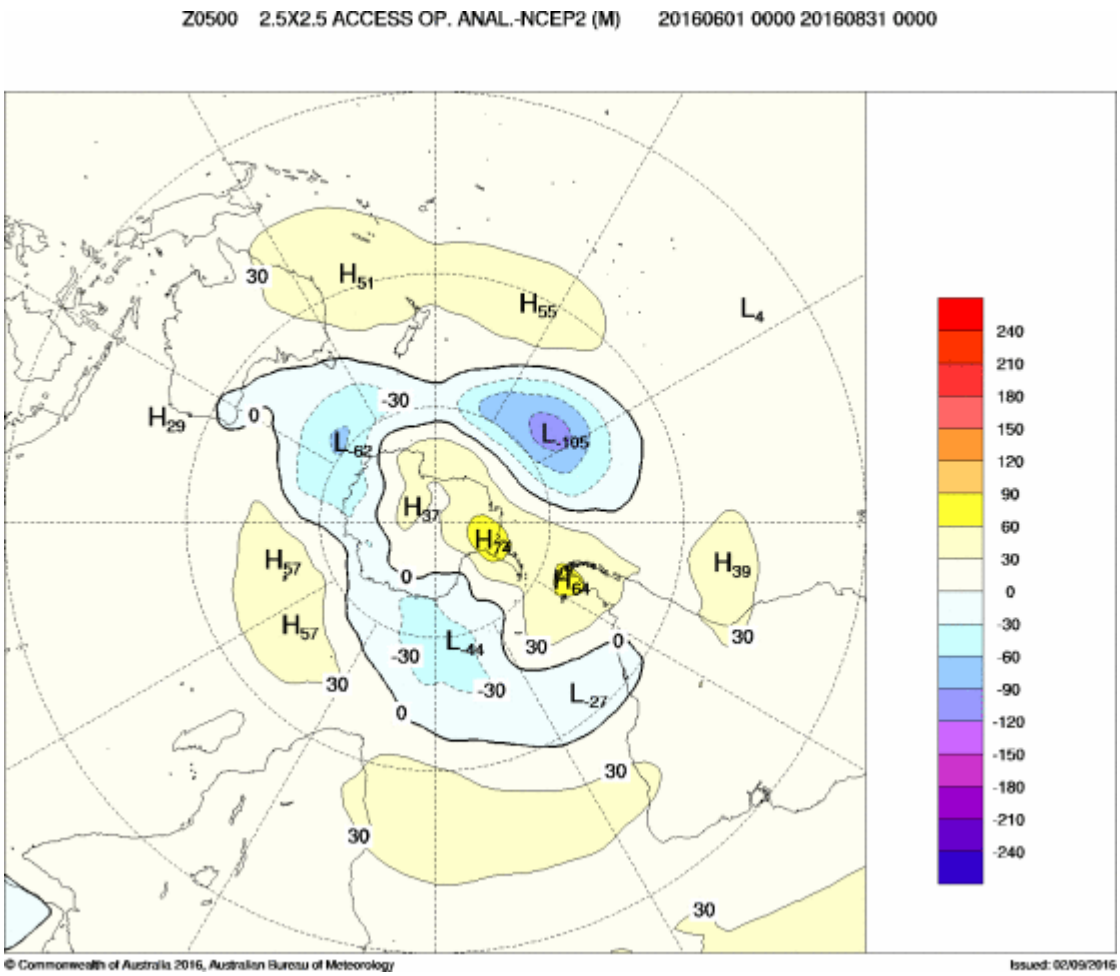

Figure 14 The 500 hPa mean geopotential height anomalies (gpm) for winter 2016, relative to 1979–2000.

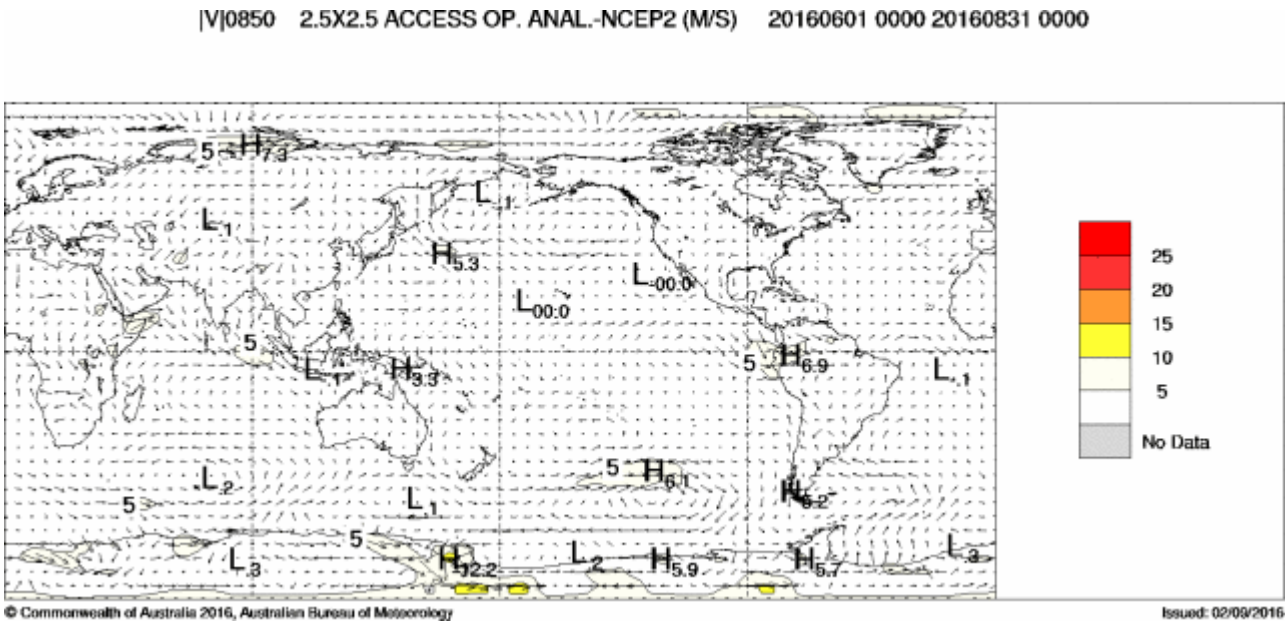

Figure 15 850 hPa vector wind anomalies (ms^{-1}) for the austral winter 2016.

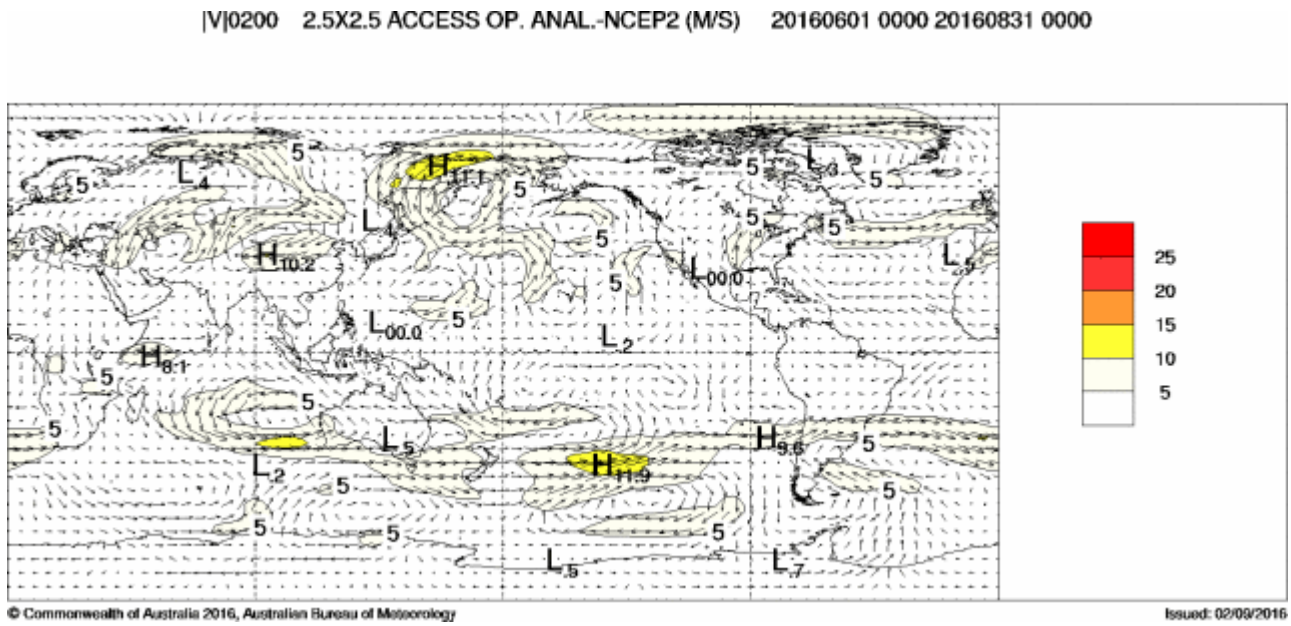

Figure 16 200 hPa vector wind anomalies (ms^{-1}) for the austral winter 2016.

9 Australian Region

9.1 Rainfall

Winter 2016 was exceptionally wet almost throughout Australia. Averaged nationally[9], it was the second-wettest winter in 117 years of record (after 1978), with seasonal rainfall 83% above the 1961-1990 average (Table 1). Apart from some seasonally dry areas of northern Australia (Figure 17a), the only substantial area not to exceed average rainfall was a section of southwest Western Australia.

The wet conditions were most extreme in Queensland, which also had its second wettest winter on record, after 1912. Substantial parts of the State had their wettest winter on record (Figure 17b), particularly in the central west, which had been suffering from severe long-term drought. Many inland areas received more than four times their average winter rainfall. Record high winter rainfall also extended to the coast between Rockhampton and Mackay. An extensive area of record winter rainfall also occurred in southern and central inland New South Wales. Winter rainfall was above the 90th percentile over most of New South Wales, and most of Queensland except for the southeast corner and Cape York Peninsula. It was also above the 90th percentile in most of Tasmania, especially the north, and large areas of the western and central interior. In total, it was the wettest winter on record over 4.2% of Australia, including 14.2% of Queensland and 8.6% of New South Wales (Table 2); rainfall was in the highest decile over 44.6% of Australia, and over two-thirds or more of Queensland, New South Wales and Tasmania.

All three months were at least 50% wetter than average for Australia. June was especially wet at 125% above average; it was the second-wettest on record nationally, and the wettest on record for New South Wales. July was particularly wet in Victoria and Tasmania. A major east-coast trough and low between 4 and 7 June brought significant flooding to many areas, particularly coastal New South Wales and northern Tasmania. A number of northern Tasmanian sites received daily totals above 200 millimetres on 6 June, setting records for any time of year. Indicating the extent of the coastal rain event in New South Wales (where 19 out of 20 coastal river basins received catchment-averaged daily totals of at least 75 millimetres), 5 June was the wettest day on record for eastern New South Wales, whilst 6 June was the wettest day on record for northern Tasmania.[10]

[9] Rainfall reported in this section is based on the Australian Water Availability Project (AWAP) dataset (Jones et al., 2009).
[10] Bureau of Meteorology, Special Climate Statement 57, *Extensive early June rainfall affecting the Australian east coast.* Available at http://www.bom.gov.au/climate/current/statements/scs57.pdf.

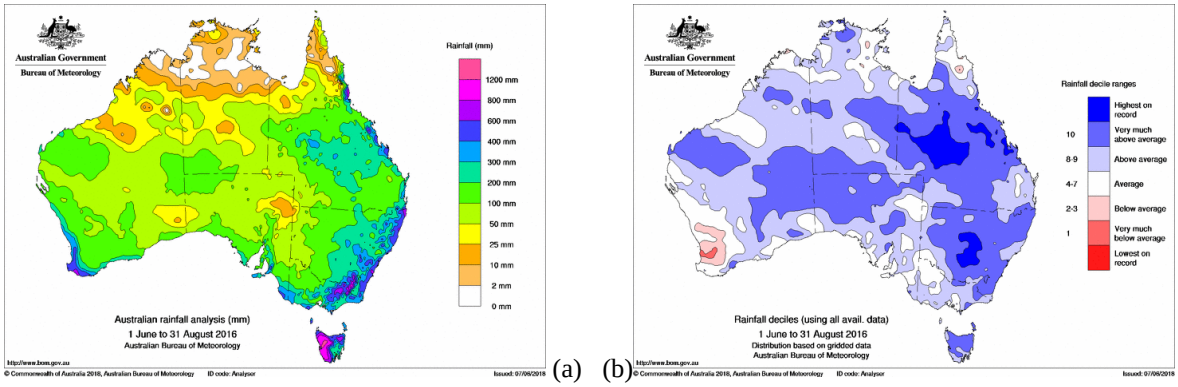

Figure 17 (a) Rainfall totals for winter 2016; (b) Rainfall deciles for winter 2016; decile ranges based on grid-point data with respect to all available data 1900–2017.

Region	*Highest seasonal total (mm)*	*Lowest seasonal total (mm)*	*Highest daily total (mm)*	*Area averaged total*	*Rank of area averaged total (mm)*	*Difference from mean (%)*
Australia	1670.6 at Bellenden Ker (Top)	zero at several locations	430.0 at Coramba (Glenfiddich) on 5 June	117.09	116	83.0%
Queensland	1670.6 at Bellenden Ker (Top)	zero at several locations	310.8 at Pacific Heights on 17 July	143.16	116	179.2%
New South Wales	1018.6 at Perisher Valley	53.6 at Tibooburra Airport	430.0 at Coramba (Glenfiddich) on 5 June	218.70	115	88.6%
Victoria	857.2 at Mt Buller	63.6 at Lindsay Point	120.2 at Reeves Knob on 7 July	251.98	99	24.0%
Tasmania	1340.2 at Gordon Power Station	142.4 at Bothwell (Clyde River)	248.0 at Yolla & Loongana on 6 June	643.07	113	46.7%
South Australia	601.0 at Uraidla	23.0 at Cameron Corner (Lindon)	99.0 at Whyalla (Mullaquana) on 18 June	93.04	110	67.3%
Western Australia	710.4 at Karri Valley Resort	zero at several locations	113.2 at Jarrahwood on 16 July	89.42	101	47.1%
Northern Territory	122.8 at Yulara Airport	zero at several locations	57.0 at Avon Downs on 19 June	41.11	103	126.2%

Table 1 Summary of the seasonal rainfall ranks and extremes on a national and State basis for winter 2016. The rank refers to 1 (lowest) to 117 (highest) and is calculated over the years 1900 to 2016 inclusive.

9.2 Rainfall deficiencies

The heavy rains of winter 2016 largely eliminated short- to medium-term rainfall deficiencies in Australia. At the start of the season (Figure 18a), there was a substantial area of rainfall deficiencies analysed over the period since May 2015 which covered most of southern Victoria from central Gippsland eastward, as well as areas south and east from Adelaide in South Australia. These deficiencies were almost entirely eliminated by the winter 2016 rainfall, with only a few residual areas remaining by the end of August, mostly in south Gippsland and around Melbourne (Figure 18b). Deficiencies also remained on this timescale in an area around Perth, and in scattered small regions in northern Australia where the deficiencies reflected below-average rainfall in the 2015-16 wet season. In the winter 2016 season itself, rainfall deficiencies for the three-month period were almost entirely confined to Western Australia (Table 2), in a small region south of Perth.

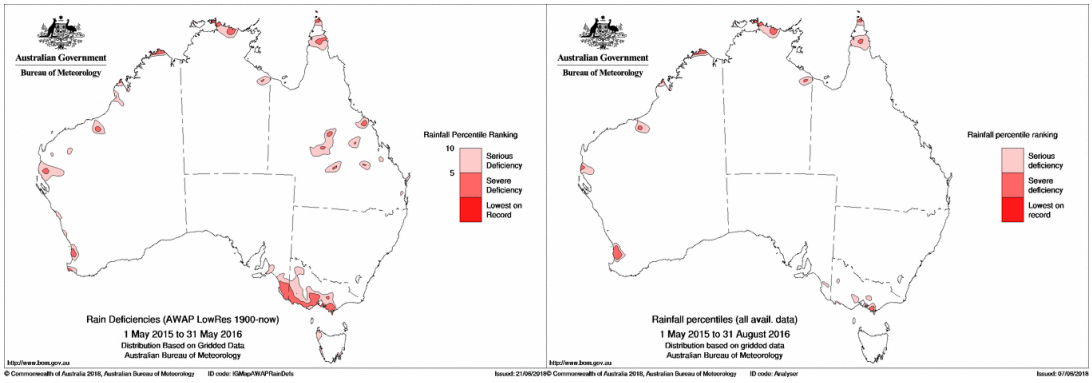

Figure 18 Rainfall deficiencies for (a, left) the 13-month period May 2015 to August 2016 and (b, right) the 16-month period May 2015 to May 2016.

Region	*Lowest on record (%)*	*Severe deficiency (%)*	*Decile 1 (%)*	*Decile 10 (%)*	*Highest on record (%)*
Australia	0.00	0.0	0.2	44.6	4.23
Queensland	0.00	0.1	0.1	68.2	14.19
New South Wales	0.00	0.0	0.0	75.1	8.58
Victoria	0.00	0.0	0.0	11.0	0.00
Tasmania	0.00	0.0	0.0	70.5	2.72
South Australia	0.00	0.0	0.0	45.2	0.07
Western Australia	0.00	0.0	0.5	28.5	0.14
Northern Territory	0.00	0.0	0.0	29.2	0.11

Table 2 Percentage areas in different categories for winter 2016 rainfall. ‘Severe deficiency’ denotes rainfall at or below the 5th percentile. Areas in decile 1 include those in ‘severe deficiency’, which in turn includes areas which are ‘lowest on record’. Areas in decile 10 include areas which are ‘highest on record’. Percentage areas of highest and lowest on record are given to two decimal places because of the small quantities involved; other percentage areas are to one decimal place.

Substantial multi-year rainfall deficiencies, which had been present since 2012, also existed at the start of the season over many parts of eastern Australia, particularly focused on two regions; one covering much of inland Queensland and extending into adjacent regions of northern inland New South Wales, the other covering central and western Victoria and southeast South Australia. The northern region of deficiencies was substantially reduced by the winter 2016 rains; the southern region remained largely unchanged in size, but substantially reduced in intensity, with most remaining lowest-on-record areas removed.

9.3 Temperature

Winter 2016 was warmer than average over the Australian region.[11] As would be expected of a wet winter, with extra cloud cover reducing nocturnal radiational cooling, the warmth was most prominent at night. Seasonally averaged minimum temperatures for Australia were 1.49 °C above the 1961-1990 average (Table 4), the fourth-warmest on record and the warmest since 1998. Whilst maximum temperatures were much closer to average, they were still above average for Australia and for all States (Table 3).

[11] National and regional temperatures in this section use the Australian Climate Observations Reference Network – Surface Air Temperature (ACORN-SAT) dataset (Trewin, 2013).

Most of Australia had overnight minimum temperatures substantially above average (Figure 20), with only the southern half of Western Australia near or slightly below average. The northern half of Australia was particularly warm, with seasonal minimum temperatures more than 2 °C above average over most of the region, reaching more than 3 °C above average in parts of south-central Queensland and the western Kimberley in Western Australia. Some regions in both States had their highest winter mean minimum temperatures on record. Most of New South Wales, Tasmania and eastern Victoria had minimum temperatures 1 to 2 °C above average, with some records set in southern New South Wales. Overnight warmth was prominent in both June and July, with both months ranking in the top five nationally; August minimum temperatures were closer to the long-term average, with an anomaly of +0.67 °C.

Maximum temperatures were generally above average in the northern tropics, along the east coast and in Tasmania (Figure 19). Elsewhere, maximum temperatures were near or below average; some parts of inland Queensland which experienced particularly heavy winter rains had seasonal maximum temperatures in the lowest decile. Maximum temperature anomalies were largest in the northern tropics, with parts of the northern Kimberley having their warmest winter on record with temperatures more than 2 °C above average. Kalumburu, in this region, set a new Australian record high temperature for July with 38.3 °C on the 24th. At the national level, all three winter months were slightly warmer than average; the warmth in northwestern Australia was most prominent in June, when maximum temperatures were up to 4 °C above average in parts of the Northern Territory.

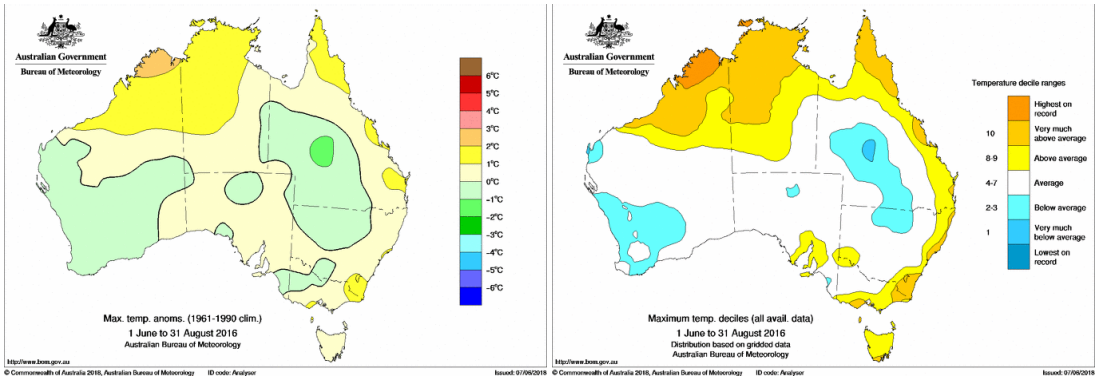

Figure 19 (a) Maximum temperature anomalies (°C) for winter 2016; based on average climate 1961–1990; (b) Maximum temperature deciles for winter 2016 from analysis of ACORN-SAT data: decile ranges based on grid-point values over the winters 1910–2017.

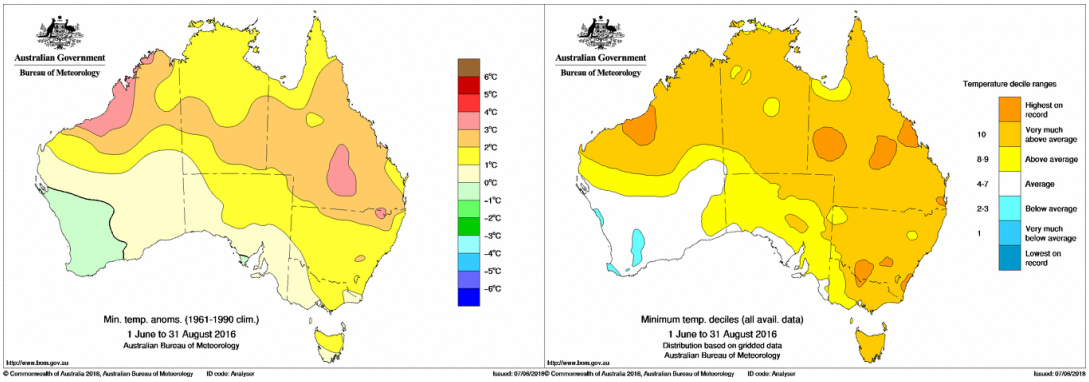

Figure 20 (a) Minimum temperature anomalies (°C) for winter 2016; based on average climate 1961–1990; (b) Minimum temperature deciles for winter 2016 from analysis of ACORN-SAT data: decile ranges based on grid-point values over the winters 1910–2017.

10 Southern Hemisphere

The austral winter of 2016 was significantly warmer than average over most parts of the southern hemisphere. Averaged over the southern hemisphere as a whole, it was one of the warmest winters on record. Of the three major global datasets, winter 2016 ranked as the warmest on record for the southern hemisphere in the National Oceanic and Atmospheric Administration (NOAA) dataset (Smith and Reynolds, 2005), equal warmest (with 2009) in the National Aeronautics and Space Administration (NASA) dataset (Hansen et al., 2010), and third warmest in the United Kingdom Meteorological Office Hadley Centre/Climatic Research Unit, University of East Anglia (HadCRU) dataset (Morice et al, 2012). The differences in ranks between the three datasets reflect the different methods they use for assessing temperatures over data-sparse land areas, particularly Antarctica, whilst the uncertainty in temperature measurements is typically greater in the southern hemisphere than the northern due to the lower data density.

Region	*Highest seasonal mean maximum (°C)*	*Lowest seasonal mean maximum (°C)*	*Highest daily maximum temperature (°C)*	*Lowest daily maximum temperature (°C)*	*Area-averaged temperature anomaly (°C)*	*Rank of area-averaged temperature anomaly*
Australia	34.4 at Kalumburu	1.3 at Thredbo AWS	38.3 at Kalumburu on 24 July	-5.8 at Thredbo AWS on 13 July	0.32	73
Queensland	32.1 at Coconut Island	15.3 at Applethorpe	35.8 at Coen on 24 August	6.8 at Applethorpe on 6 July	0.10	62
New South Wales	22.2 at Casino	1.3 at Thredbo AWS	31.0 at Casino on 9 June	−5.8 at Thredbo AWS on 13 July	0.13	59
Victoria	16.6 at Mildura	1.9 at Falls Creek	26.0 at Mildura on 18 August	−4.6 at Mt Hotham on 24 June & 13 July	0.38	77=
Tasmania	14.8 at Bicheno	3.8 at kunanyi (Mt Wellington)	20.0 at Swansea on 19 August	−3.6 at kunanyi on 23 July	0.41	89
South Australia	20.2 at Oodnadatta	10.4 at Mt Lofty	30.1 at Coober Pedy on 18 August	4.6 at Mt Lofty on 12 July	0.15	54=
Western Australia	34.4 at Kalumburu	13.9 at Katanning	38.3 at Kalumburu on 24 July	8.8 at Rocky Gully on 8 August	0.27	64=
Northern Territory	34.3 at Oenpelli & Middle Point	20.5 at Arltunga	37.9 at Middle Point on 25 August	10.0 at Arltunga on 13 July	0.95	95

Table 3 Summary of the mean seasonal maximum temperatures, extremes and rank for Australia and Regions for winter 2016. Rank given is 1 (lowest) to 107 (highest) calculated, over the years 1910 to 2016 inclusive.

Temperatures in winter 2016 were above the long-term average over most southern hemisphere land areas outside Antarctica, with the only substantial areas with temperatures below the 1981-2010 average being an area of east-central South America (centred on northern Argentina, Paraguay and parts of southern Brazil) and the southwest of Western Australia (Figure 21). Much of southern Africa, particularly the western half, had winter mean temperatures 1 °C or more above average, with much of the region analysed in global data sets as having its warmest winter on record. Temperatures 1 °C or more above average also covered parts of northern Brazil, northern Australia and the Antarctic Peninsula. New Zealand had winter mean temperatures 0.6 °C above the 1981-2010 average, its eighth warmest winter on record (NIWA, 2016). The Antarctic interior experienced temperatures well below average in July but well above average in August; mean monthly temperature anomalies at the South Pole were approximately −4 °C in July and +4 °C in August.

Region	*Highest seasonal mean minimum (°C)*	*Lowest seasonal mean minimum (°C)*	*Highest daily minimum temperature (°C)*	*Lowest daily minimum temperature (°C)*	*Area-averaged temperature anomaly (°C)*	*Rank of area-averaged temperature anomaly*
Australia	24.9 at Coconut Island	−3.3 at Thredbo AWS	28.8 at Troughton Island on 6 June	−10.4 at Thredbo AWS on 7 August	1.49	104
Queensland	24.9 at Coconut Island	3.7 at Stanthorpe	27.0 at Coconut Island on 2 June	−4.5 at Stanthorpe on 26 June & 30 July	2.37	106
New South Wales	13.5 at Cape Byron	−3.3 at Thredbo AWS	18.4 at Mungindi on 21 July	−10.4 at Thredbo AWS on 7 August	1.66	107
Victoria	9.6 at Wilsons Promontory	−2.0 at Falls Creek	15.9 at Moorabbin on 19 August	−8.0 at Mt Hotham on 13 & 14 July	0.91	100
Tasmania	9.3 at Swan Island	−1.1 at Liawenee	15.9 at Flinders Island Airport on 5 June	−9.0 at Liawenee on 1 June	1.06	104
South Australia	11.8 at Neptune Island	4.2 at Hawker	16.9 at Oodnadatta on 29 August	−5.0 at Yunta on 16 July	0.99	96
Western Australia	24.8 at Troughton Island	3.6 at Wandering	28.8 at Troughton Island on 6 June	−4.0 at Eyre on 13 August	0.98	101
Northern Territory	24.8 at McCluer Island	6.5 at Arltunga & Alice Springs	27.6 at McCluer Island on 4 June	−4.5 at Kulgera on 16 July	1.70	101

Table 4 Summary of the mean seasonal minimum temperatures, extremes and rank for Australia and Regions for winter 2016. Rank refers to 1 (lowest) to 107 (highest) calculated, over the years 1910 to 2016 inclusive[12].

[12] A subset of the full temperature network is used to calculate the spatial averages and rankings shown in Table 3 (maximum temperature) and Table 4 (minimum temperature); this dataset is known as ACORN-SAT (see http://www.bom.gov.au/climate/change/acorn-sat/ for details). These averages are available from 1910 to the present. As the anomaly averages in the tables are only retained to two decimal places, tied rankings are possible. Rankings marked with "=" denote tied rankings. ACORN-SAT temperatures are also used for Table 5.

Figure 22 shows global rainfall patterns for the June to August period. Much of southern South Africa had winter rainfall 50% or more above average, although rainfall was close to average in the Western Cape. Other parts of southern Africa were generally seasonably dry. In South America, notable dry regions included northeast Brazil, where significant drought continued, whilst long-term drought also continued in parts of the Amazon basin, particularly its west, despite winter rainfall anomalies being unexceptional. It was also significantly drier than normal in much of central and southern Chile from the Santiago region southwards, extending into the far south of Argentina. Other parts of Argentina saw generally average to above-average rainfall.

After large El Niño-related rainfall anomalies in earlier seasons, the islands of the South Pacific saw generally near-average rainfall in winter 2016. Precipitation was also generally close to average in New Zealand, except for an area of above-average values in the Hawke's Bay region of the North Island and below-average values on the east coast of the South Island from Christchurch northwards. It was a wet June-August in many parts of Indonesia, particularly Java and the islands east of Java, where sea-surface temperatures were at or near record levels (Figure 9); the negative Indian Ocean Dipole phase may also have had an influence.

Region	*Maximum temperature*				*Minimum temperature*			
	Lowest on record	*Decile 1*	*Decile 10*	*Highest on record*	*Lowest on record*	*Decile 1*	*Decile 10*	*Highest on record*
Australia	0.00	0.3	17.4	1.40	0.00	0.0	66.9	5.10
Queensland	0.00	1.4	11.4	0.00	0.00	0.0	96.1	13.07
New South Wales	0.00	0.0	7.6	0.00	0.00	0.0	92.9	6.99
Victoria	0.00	0.0	11.2	0.00	0.00	0.0	60.9	2.99
Tasmania	0.00	0.0	7.9	0.00	0.00	0.0	100.0	0.00
South Australia	0.00	0.0	0.0	0.00	0.00	0.0	25.1	0.00
Western Australia	0.00	0.1	18.4	4.20	0.00	0.0	42.8	3.99
Northern Territory	0.00	0.0	44.3	0.17	0.00	0.0	89.1	0.00

Table 5 Percentage areas in different categories for winter 2016. Areas in decile 1 include those which are ‘lowest on record’. Areas in decile 10 include areas which are ‘highest on record’. Percentage areas of highest and lowest on record are given to two decimal places because of the small quantities involved; other percentage areas are to one decimal place.

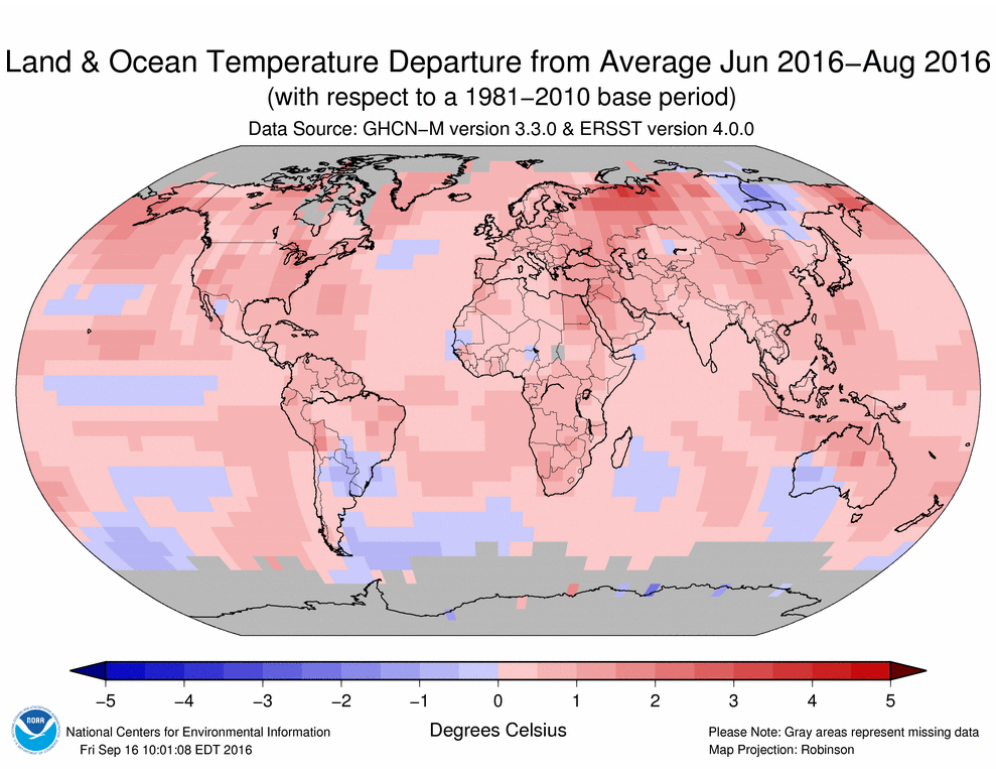

Figure 21 Mean temperature anomalies (°C) from a 1981-2010 base period for June to August 2016 (source: National Centers for Environmental Information).

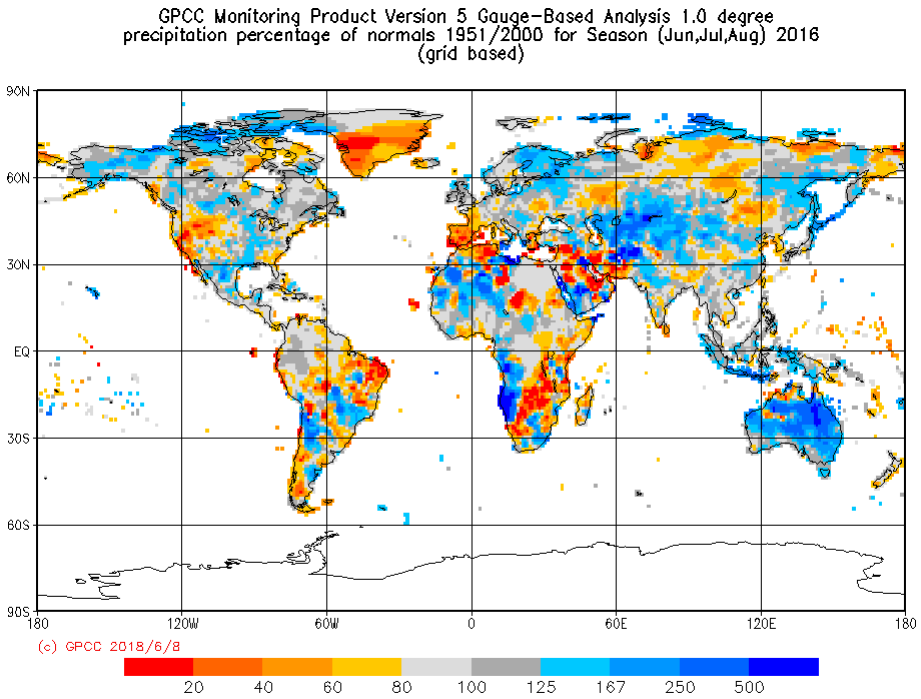

Figure 22 Precipitation as a percentage of the 1951-2000 average for June to August 2016 (source: Global Precipitation Climatology Centre).

Acknowledgements

Thanks to Catherine Ganter and Robert Fawcett for their helpful comments on the manuscript.

References

Donald, A. et al., 2004. *Forecasting with the Madden-Julian Oscillation and the applications for risk management.* Brisbane, 4th International Crop Science Congress, 2004.

Hansen, J., Ruedy, R., Sato, M. and Lo, K. 2010. Global surface temperature change. *Rev. Geophys*, 48, RG4004, doi: 10.1029/2010RG000345.

Hendon, H., Thompson, D.W.J. and Wheeler, M.C., 2007. Australian rainfall and surface temperature variations associated with the southern hemisphere annular mode. *J. Climate*, 20, 2452-2467.

Huang, B. and coauthors. 2017. Extended Reconstructed Sea Surface Temperature, Version 5 (ERSSTv5): upgrades, validations and intercomparisons. *J. Climate*, 30, 8179-8205.

Jones, D.A., Wang, W. and Fawcett, R. 2009. High-quality spatial climate data-sets for Australia. *Aust. Met. Oceanogr. J.*, 58, 233-248.

Kanamitsu, M. Ebisuzaki, W., Woollen, J., Yang, S.-K, Hnilo, J.J., Fiorino, M. and Potter, G.L., 2002. NCEP-DOE AMIPII Reanalysis (R-2). *Bull. Amer. Met. Soc.*, 83, 1631–1643.

Kuleshov, Y., Qi, L., Fawcett, R. and Jones, D., 2009. Improving preparedness to natural hazards: Tropical cyclone prediction for the Southern Hemisphere. *Advances in Geosciences*, Vol. 12(Ocean Science), 127-143.

Madden, R. A. and Julian, P. R., 1971. Detection of a 40-50 day oscillation in the zonal wind in the tropical Pacific. *J. Atmos. Sci.*, 28, 702-708.

Madden, R. A. and Julian, P. R., 1972. Description of global-scale circulation cells in the tropics with a 40-50 day period. *J. Atmos. Sci.*, 29, 1109-1123.

Madden, R. A. and Julian, P. R., 1994. Observations of the 40-50 day tropical oscillation: a review. *Mon. Wea. Rev.*, 122, 814–837.

Morice, C.P., Kennedy, J.J., Rayner, N.A. and Jones, P.D. 2012. Quantifying uncertainties in global and regional temperature change using an ensemble of observational estimatesL the HadCRUT4 dataset. *J. Geophys. Res.*, 117, D08101, doi: 10.1029/2011JD017187.

Rosemond, K. and Tobin, S. 2018. Seasonal climate summary for the southern hemisphere (autumn 2016): El Niño slips into neutral and a negative Indian Ocean Dipole develops. *J. South. Hem. Earth Sys. Sci.*, in press.

Saji, N.H., Goswami, B.N., Vinayachandran, P.N., and Yamagata, T. 1999. A dipole mode in the tropical Indian Ocean. *Nature*, 401, 360-363.

Smith, T.M. and Reynolds, R.W. 2005. A global merged land air and sea surface temperature reconstruction based on historical observations (1880-1997). *J. Climate*, 18, 2021-2036.

Trewin, B.C. 2013. A daily homogenized temperature data set for Australia. *Int. J. Climatol.*, 33, 1510-1529.

Troup, A., 1965. The Southern Oscillation. *Quart. J. Royal Met. Soc.*, 91, 490-506.

Wang, G. and Hendon, H. H., 2007. Sensitivity of Australian rainfall to inter-El Niño variations. *J. Climate*, 20, 4211-4226.

Wheeler, M. and Hendon, H., 2004. An All-Season Real-Time Multivariate MJO Index: Development of an Index for Monitoring and Prediction. *Mon. Wea. Rev.*, 132, 1917-1932.